Volume 9, Issue 6, 2019, 4635 - 4641 ISSN 2069-5837

Biointerface Research in Applied Chemistry

www.BiointerfaceResearch.com

https://doi.org/10.33263/BRIAC96.635641

Original Research Article Open Access Journal

Received: 05.10.2019 / Revised: 16.11.2019 / Accepted: 18.11.2019 / Published on-line: 20.11.2019

Synthesis, characterisation, and application of chamomile gold nanoparticles in molecular diagnostics: a new component for PCR kits

Mohammad Jafar Maleki [1], Mohammad Pourhassan-Moghaddam [1,*], Abbas Karimi [2], Abolfazl Akbarzadeh [3, 4], Nosratollah Zarghami [1], Seyed Abolghasem Mohammadi [1,*]

[1]Department of Medical Biotechnology, Faculty of Advanced Medical Sciences, Tabriz University of Medical Sciences, Tabriz, Iran
[2]Department of Molecular Medicine, Faculty of Advanced Medical Sciences, Tabriz University of Medical Sciences, Tabriz, Iran
[3]Department of Medical Nanotechnology, Faculty of Advanced Medical Sciences, Tabriz University of Medical Sciences, Tabriz, Iran
[4]Department of Chemical Engineering, Northeastern University, Boston, MA, 02115 USA

*corresponding author e-mail address: ***mohammadi@tabrizu.ac.ir; pourhassanm@tbzmed.ac.ir*** | Scopus ID 35606114800; Scopus ID 55181898000

ABSTRACT

Various strategies have been suggested for successful amplification of the hard-to-amplify nucleic acids such as the inclusion of various chemical or biological materials in the in vitro nucleic acid amplification reactions, particularly polymerase chain reaction (PCR), and adjustment of the cycling programs. Although much efforts have been madefor improvements in the enhancement of polymerase chain reactions of high GC content nucleic acids, still significant challenges remain. In this study, the effects of citrate-coated AuNP and chamomile extract-coated AuNP (p-AuNP) on amplification of three genes with significant different GC percentage were evaluated. Owing to the enormous potential of gold nanoparticles in the enhancement of the PCR reactions, we showed the promising and consistent findings on the application of very dilute biocompatible chamomile-gold nanoparticles as safe and low-cost nanomaterials for molecular amplification of GC-rich DNA samples. We hypothesized that green AuNPs, which have different surface chemistry from cit-AuNPs, not only do not interfere with the PCR reactants but also are capable of enhancing PCR reactions. These results, for the first time, confirm the potential of using the green gold nanoparticles in the heat-assisted enzymatic in vitro reactions, suggesting Chamomile gold nanoparticles as reliable component of any PCR kits.

Keywords: *green gold nanoparticles; polymerase amplification; in vitro diagnostics; molecular assays.*

1. INTRODUCTION

The enzymatic amplification of GC-rich DNA has been proven as a technically challenging and non-reproducible task in genomics and molecular diagnosis procedures [1, 2]. Thus, various strategies have been applied to address this problem. In some approaches, the amplification program is modified to include several extra cycling steps [3-6]. Although these methods have resulted in promising improvements in the PCR results, there is still a need for adding some chemicals, especially 7-deaza-2′-deoxyguanosine 5′-triphosphate, in the amplification reaction [7].

Due to customizing the amplification program, these methodologies are not suitable for performing multiplex and quantitative PCR (qPCR) experiments; because the programme of the PCR cycles does not remain constant throughout the PCR and the cycles progress in an unorganized manner. Thus, the exponential phase, which is required for quantification of the results, does not occur in PCR reactions with the extra cycling steps [3-6, 8]. Therefore, any attempt to improve the amplification of GC-rich nucleic acids should not hinder performing multiplex and qPCR reactions. Moreover, the inclusion of the additional cycling steps makes the amplification procedure time-intensive and costly [3-6, 8].

In the reagent-dependent approaches of GC-rich DNA amplification, various types of chemical and biological materials have been added to the amplification reactions as enhancers [8-14]. Mechanistically, in these approaches, the added enhancers intensify the amplification reactions through different ways including stabilizing the DNA polymerase and increasing the DNA denaturation which speeds up the progression of cycles. The advantage of using additives is that modification of the standard amplification programs is not required. Nonetheless, most of these additives are proven to be toxic materials. Furthermore, some of them have exhibited unexpected effects on PCR, when used in high concentrations. For example, it has been shown that the excess DMSO can reduce the annealing temperature of primers; which in turn increases the chances of mispriming [7]. Also, these additives may denature DNA polymerases that are used in PCR [7], leading to decreasing the efficiency of amplification.

Some of PCR additives can interfere with the post-PCR procedures such as visualization of the amplicons. For instance, 7-deaza-2′-deoxyguanosine 5′-triphosphate reduces the rate of ethidium bromide staining of DNA [7]. Bovine serum albumin (BSA) as a protein additive, enhance the effect on PCR through reversing the effect of PCR inhibitors, in some cases, it also exhibits inhibitory effects [15, 16].

Due to the limitations of the current additives, nanomaterials particularly gold nanoparticles (AuNPs) have been introduced as alternative enhancers namely nano-enhancers. The logic behind the application of AuNPs as nano-enhancers is their easy preparation, high stability and excellent heat transfer properties [17]. While in the reaction, AuNPs evenly distribute the heat toward all directions of the reaction and may boost the enzymatic amplification of DNA by efficient denaturation of DNA strands [18]. Although enhancement of PCR reactions has been reported by citrate-AuNPs (cit-AuNPs), there is evidence of PCR inhibition by cit-AuNPs which can be reversed by blocking their surface with BSA [18-20]. The reason underlying these discrepant

reports is mainly attributable to the denaturation and inhibition of DNA polymerase by the cit-AuNPs through non-reversible adsorption of DNA polymerase to the surface of these AuNPs [20]. Therefore, to obtain reproducible enhancement of PCR reactions, there is a need for the use of AuNPs that possess alternative surface composition. We hypothesized that green AuNPs, which have different surface chemistry from cit-AuNPs, not only does not interfere with the PCR reactants but also are capable of enhancing PCR reactions. In other words, the excellent biocompatibility of green AuNPs allows them to interact with the PCR components without destroying/modifying their role and their highly conductive core distributes the heat efficiently, which leads to a homogenous thermal cycling condition.

Taken together, in this work, we have developed a facile and highly reproducible method for fabrication of green biocompatible AuNPs using Chamomile extract as a source of natural reductants, followed by successful application of only a very dilute solution of the fabricated green AuNPs in GC content-dependent enhancement of PCR reactions.

2. MATERIALS AND METHODS

2.1. Chemical synthesis of AuNPs.

Citrate AuNPs (cit-AuNPs) were prepared based on the Turkevich method [21]. Briefly, 10 mL HAuCl4 (1 mM) was heated at 120 °C to boiling while being stirred at 1000 rpm. Then, 1 mL trisodium citrate (1 mM) was added quickly to the boiling HAuCl4 solution, and the mixture was incubated for 10 min for development of the deep-red colour solution. After that, the heat was turned off while stirring was continued until the solution cooled down. The resultant solution was kept in the dark until further use.

2.2. Green synthesis of AuNPs.

2.2.1. Preparation of total extract.

Total extract of Matricaria chamomilla was prepared by soaking 10g of the dried plant in 400 mL MQ water, followed by boiling for 20 min and filtration of the boiled material by Whatman paper no. 2. The filtrate was allowed to dry for one week in the dark at 50 °C. Following weighing, a solution of 20 mg/mL extract was prepared. This solution was used as a reductant for p-AuNP synthesis [22, 23].

2.2.2. Synthesis.

Plant AuNPs (p-AuNPs), also known as Chamomile AuNPs, were prepared by reduction of 1 mM of Au3+ solution with Total Extract of Matricaria Chamomilla (TEMC) at different conditions including different ratios, temperatures, and the pH values while shaking at 130 rpm. Different ratios of Au3+ solution/TEMC (3:1, 4:1, 5:1 and 6:1) were treated at three different temperatures, namely 25, 60 and 97 °C while shaking at 130 rpm. The effect of the pH on AuNP formation was studied by performing the synthesis reactions in three different pH values; namely real pH of the reaction, 7 and 12 [22, 23].

2.2.3. Characterisation.

The formations of as-prepared AuNPs were monitored using colour change, ultraviolet–visible (UV-VIS) spectrophotometry, Transmission electron microscopy (TEM) and Fourier-transform infrared spectroscopy (FTIR). Also, biocompatibility of the prepared AuNP solutions was studied in vitro. Any colour change was monitored using the naked eye during the synthesis of AuNP solutions. The L-SPR curve of AuNPs was recorded in the range of 400-900 nm using Bioaquarius spectrophotometer (CE7250 model, from CECIL Co.) to determine the maximum extinction wavelength and concentration of the as-prepared AuNP solutions. Concentrations of the AuNPs were calculated considering the absorbance of the AuNP solutions at 450 nm (OD450) by following the protocol provided elsewhere [24]. TEM was used for the study of size and morphology of AuNPs using, and the TEM images were analyzed using ImageJ version v1.52d (NIH, USA).

In order to confirm the incorporation of TEMC biomolecules in p-AuNPs during their bioreduction, FTIR analysis was used. A TEMC sample was included as the reference. Furthermore, to evaluate the eco-friendliness and biocompatibility, cit-AuNPs and p-AuNPs were separately exposed to E.coli and human MCF-7 cells (C135, Pasteur Institute of Iran), as ecological and biocompatibility models. Any changes in the viability of *Escherichia coli* and MCF-7 cells were recorded using pour-plate colony count method [25] and MTT-assay [22], respectively.

2.3. Evaluation of the effect of the as-prepared AuNPs on in vitro polymerase reactions.

Polymerase Chain Reaction (PCR) was used as a model reaction to mimic the effect of as-prepared AuNPs.

2.3.1. DNA extraction.

Total human DNA was extracted from 10 mL heparinized blood from a healthy sample, provided by a male subject after obtaining his consent, using the simple salting-out method with slight modifications [26]. Briefly, the blood was centrifuged in 3000 rpm for 20 min at room temperature. Then the plasma was discarded, and the pellet was resuspended in 5 mL of MQ water to lyse red blood cells (RBC). The centrifugation and lysis were repeated four times to remove any residues of RBCs completely. Then, the collected WBCs were resuspended in 3 mL of nuclei lysis buffer (10 mM Tris-HCl, 400 mM NaCl and 2 mM Na2EDTA, pH 8.2) and 1 mL of protein digestion solution containing 1mg protease K in 1% SDS and 2 mM Na2EDTA. Then, the solution was incubated at 37°C overnight, followed by addition of 5 mL of 6 M NaCl solution. The resultant solution was shaken vigorously for 30 s and centrifuged at 3000 rpm for 20 min. The supernatant was carefully transferred to a new container, and 3 mL absolute ethanol was added. After 5 times brief inversion, the solution was centrifuged in 13000 rpm for 15 min. After centrifugation, the supernatant was removed, and the pellet washed thrice with absolute ethanol. The final pellet was dissolved in 1 mL sterile water. MecA-positive bacterial DNA samples were kindly provided by Dr. Mortaza Milani (Faculty of Advanced Medical Sciences, Tabriz University of Medical Sciences).

Concentration and purity of the DNA samples were analyzed by NanoDrop ND 2000 spectrophotometer (Thermofisher Inc.) and were stored at 4°C until use.

2.3.2. Primer selection.

Primers of Human Beta-actin gene and bacterial MecA gene were designed using the online software (https://www.genscript.com/tools/pcr-primers-designer). The

primers used for amplification of the human BRAF gene were adopted from the literature [27]. The specificity and sequence features of the used primers (table 1) were checked using primer-blast (https://www.ncbi.nlm.nih.gov/tools/primer-blast/) and oligoanalyzer online tools (https://sg.idtdna.com/calc/analyzer), respectively. The GC% of products were calculated online (http://www.endmemo.com/bio/gc.php), the primers were supplied by Bioneer Inc.

2.3.3. End-point PCR.

End-point PCR reactions were performed on the DNA samples in a mixture (final volume: 20 µL) comprised of the master mix, provided by Sinaclon Inc., (10µl), forward and reverse primers 0.5µl each), DNA (2µl) and various concentrations of AuNPs. The cycling program consisted of a primary denaturation for 5 min at 94°C (1cycle); secondary denaturation at 94°C for 30 s, annealing for 30 s at different temperatures (45°C for MecA, 56°C for beta-actin, and for 62°C BRAF) and extension at 72°C for 30s (35 cycles), followed by an additional extension step at 72°C for 10 min. The PCR products were resolved using 1% agarose gel electrophoresis. Any effect on the PCR reaction was judged by comparing the intensities of the control and test reactions.

2.3.4. Real-time PCR.

The real-time PCR reactions were performed in a MIC Thermocycler (MIC Inc.) with a final volume of 12 µl containing 6 µl SYBR Green master mix (2X Greenstar, Bioneer Inc.), 1µl of each primer and 1µl of DNA and various concentrations of AuNPs. The cycling program was as follows: initial denaturation at 95°C for 15 min (1 cycle), followed by 40 cycles of denaturation at 95°C for 20 s, at different temperatures (45°C for MecA, 56°C for beta-actin, and for 62°C BRAF) and extension at 72°C for 30 s. Any effect of the AuNPs was analyzed by comparing the Ct of the control and the test reactions. For estimation of the quantity of the effect of AuNPs on real-time PCR reaction, the following formula was used:

The quantity of effect=Ct of test experiment−Ct of control experiment

In addition, the effect of AuNPs on the specificity of real-time PCR reactions was evaluated by analysis of the melting curve.

Table 1. The elected primers used in this study.

Designation	Sequence (5'>3')	Tm (°C)	CG (%)	Length (base)	CG of product (%)
Beta-actin-F	TCCCTGGAGAAGAGCTACG	55.7	57.9	19	60
Beta-actin-R	GTAGTTTCGTGGATGCCACA	55.2	50	20	
MecA-F	AGATAAAGGAATGGCTAG	45.4	38.9	18	31
MecA-R	CACTTTCAACATACAATGA	45.2	31.6	19	
BRAF-F	CTCGGTTATAAGATGGCGGCGCTGA	62.7	56	25	75
BRAF-R	AGTCGGGAGGGCGGCAGGGT	68.7	75	20	

3. RESULTS

3.1. Synthesis and characterisation of AuNPs.

cit-AuNPs did showed a non-spherical morphology with a size of ~25 nm. According to the UV-VIS spectroscopy, the as-prepared nanoparticles showed a maximum extinction at 525 nm (figure 1).

In order to obtain the optimum synthesis reaction, p-AuNPs were prepared in different synthesis conditions. Chang in synthesis pH to the basic values resulted in the production of unstable AuNPs indicated by aggregates and dark purple colour as well as changing the typical LSPR curve of the nanoparticles as pH increased to 12 (figure 2Aa). According to the analysis of UV-VIS data, the best synthesis condition was obtained by 1:5 ratio of HAuCl4: TEMC (concentration=25 mg/mL), pH 4.8 and reaction temperature of 97°C (figure 2Ab). These resultant p-AuNPs were used in PCR experiments. Moreover, in all reaction ratios, the reaction rate was increased dramatically as the reaction temperature increased (inset in figure 2Ab).

TEM graphs indicated the produced p-AuNPs had a more spherical shape as well as a narrower size range (figure 2B). However, as indicated in figure 1b, cit-AuNPs showed a less regular morphology and a dispersed size.

FTIR analysis indicated incorporation of bioactive compounds of Matricaria chamomilla in the chemical structure of p-AuNPs as stabilising and reducing molecules (figure 2C). The biocompatibility of cit-AuNPs and p-AuNPs were studied on standard bacteria and human cells in vitro to assess their biological properties. As indicated in figure 3A, the tested cit- and p-AuNPs did not show any anti-growth effects on the bacteria. However, we observed a cytotoxic effect of cit-AuNPs on MCF-7 cells in comparison to p-AuNPs (figure 3B).

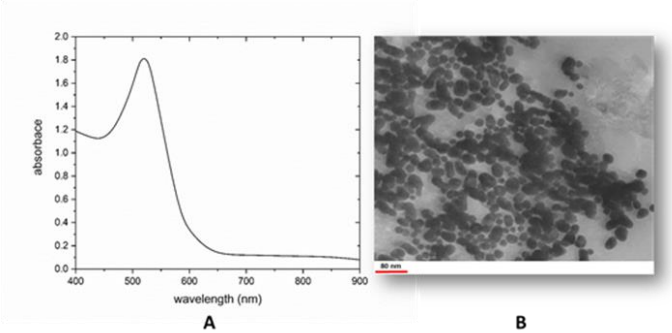

Figure 1. LSPR curve (A) and TEM graph (B) of cit-AuNPs. An absorbance peak is observed at ~525nm. In addition, the as-prepared cit-AuNPs show a varied size and morphology.

3.2. Effect of the as-prepared AuNPs on the endpoint and real-time PCR.

The quantity and purity of the DNA samples were analyzed by NanoDrop ND2000 spectrophotometer, the A260/280 was reordered greater than 1.8, indicating the high purity, and the samples were diluted to have a concentration of ~400ng/ µL.

Serial dilutions of the washed cit-AuNPs (once centrifugation at 10000 rpm for 15 min and twice centrifugation at 7000 rpm for 10 min) were included in the PCR reactions for amplification of beta-actin gene (GC content of 60%), followed by agarose gel electrophoresis. As it is indicated in figure 4, as the concentration

of cit-AuNPs increased, the bands were faded indicating inhibition of the PCR reaction by these nanoparticles (figure 4A).

As the cit-AuNPs inhibit PCR reaction, their effect was not further studied on real-time PCR reactions. In some concentrations, however, p-AuNPs could enhance the end-point PCR reactions of the beta-actin gene with a maximum enhancement in concentration OD450=0.01940625 (figure 5). Despite the p-AuNPs pellet, the supernatant phase of the p-AuNPs inhibited the PCR reaction. The result indicates that the washing steps are required for the enhancement of PCR reactions by p-AuNPs.

Analysis of the intensity of the PCR products with GelAnalyzer showed a 112% and 135% enhancement in the reactions treated with the OD450=0.0388125 and OD450=0.01940625 concentrations of p-AuNP, respectively.

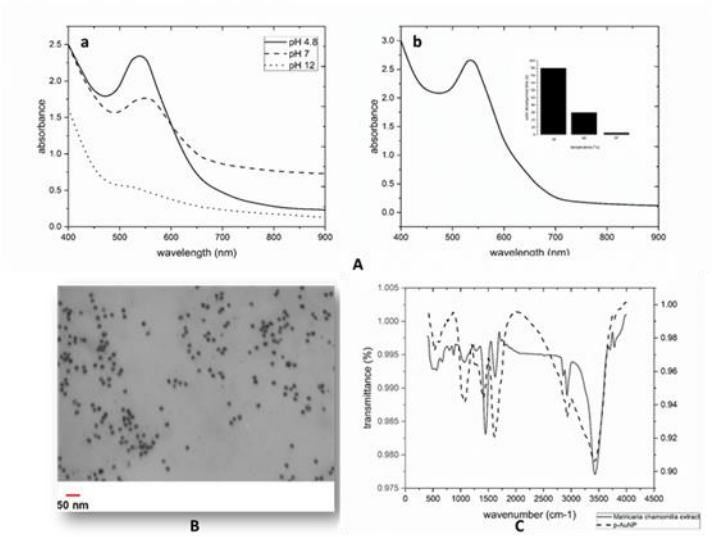

Figure 2. Main physicochemical of the synthesized p-AuNPs. A: Effect of different synthesis pH on LSPR of p-AuNPs (a). In the optimum condition (pH 4.8), absorbance was notified for the as-prepared p-AuNPs. Effect of the different temperature on the speed of p-AuNP formation at the optimum pH in which an apparent increase in the reaction speed was observed for the higher synthesis temperatures (b). B: TEM photograph of the p-AuNPs. Homogenously distributed spherically and narrow-sized AuNPs were observed, indicating the highly efficient synthesis of p-AuNPs by TEMC. C: FTIR analysis of p-AuNPs. The similar pattern of transmittance for TEMC and p-AuNPs indicates the incorporation of TEMC compounds in the structure of the p-AuNPs.

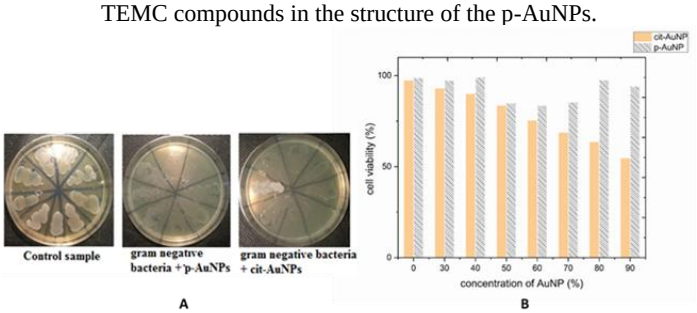

Figure 3. Biocompatibility of cit- and p-AuNPs on the E. coli (A) and MCF-7 cell line (B). p-AuNPs did not have any cytotoxic effects; however, cit-AuNPs have reduced the viability of MCF-7 cells.

In order to study the relationship between the GC content of PCR products and the enhancing level of p-AuNPs, further experiments with endpoint-PCR amplification of products containing higher GC content were carried out. BRAF gene was amplified using the end-point PCR, including a concentration range of p-AuNPs. The agarose gel electrophoresis of the resultant products (with ~75% GC) showed very sharp PCR bands for the reactions containing concentrations OD450=0.01940625 and OD450=0.009703125, while almost no band was observable for the control reaction (figure 6). The image analysis with GelAnalyzer showed that the reactions containing p-AuNP of OD450=0.01940625 resulted in 112% amplicon production.

In addition to a high GC content DNA template, an AT-rich region from bacterial mecA gene (GC content of ~31%) was amplified. The electrophoresis, as expected, showed a negligible effect of various concentrations of p-AuNPs on the PCR reactions. As it is shown in figure 7, the PCR bands possess similar intensities, confirming the GC content-dependent effect of p-AuNPs on endpoint PCR.

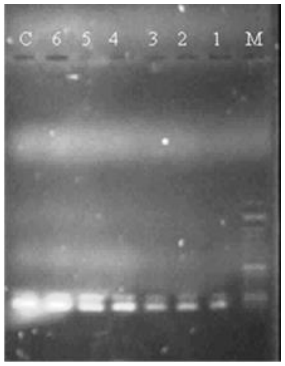

Figure 4. The inhibitory effect of cit-AuNPs on end-point PCR of beta-actin gene. M: size marker (50bp), 1: OD450=0.9, 2: OD450=0.09, 3: OD450=0.009, 4: OD450=0.0009, 5: OD450=0.00009, 6: OD450=0.000009, C: no AuNP. As the concentration of cit-AuNP increased PCR reaction was inhibited that indicates a concentration-dependent inhibition of PCR by cit-AuNPs.

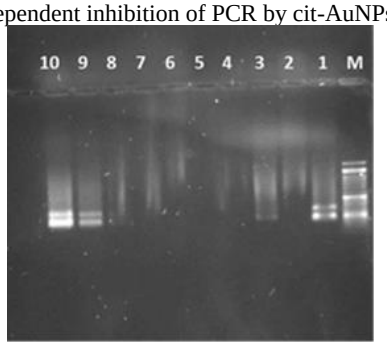

Figure 5. Effect of cit-AuNPs, p-AuNPs and p-AuNPs supernatant on end-point PCR of beta-actin gene. 1: (Control): no AuNP, 2: cit-AuNP (OD450=0.9), 3: 3.5 µL cit-AuNP (OD450=0.9)+3.5 µL H2O, 4: 7 µL Supernatant of p-AuNP, 5: p-AuNP (OD450=0.621), 6: p-AuNP (OD450=0.3105), 7: p-AuNP (OD450=0.15525), 8: p-AuNP (OD450=0.077625), 9: p-AuNP (OD450=0.0388125), 10: p-AuNP (OD450=0.01940625). In the last two concentrations, significant enhancement of beta actin gene was observed, while other concentrations inhibited the PCR reaction.

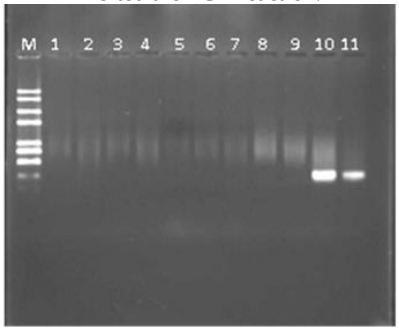

Figure 6. Effect of p-AuNPs on end-point PCR of BRAF gene. 1&2: (Controls): no p-AuNP, 3: OD450=2.484, 4: OD450=1.242, 5: OD450=0.621, 6: OD450=0.3105, 7: OD450=0.15525, 8: OD450=0.077625, 9: OD450=0.0388125, 10: OD450=0.01940625, 11: OD450=0.009703125.

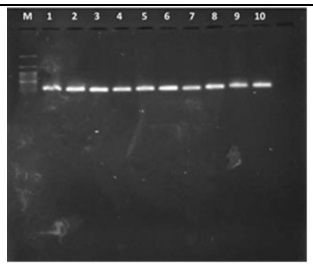

Figure 7. Effect of p-AuNPs on end-point PCR of mecA gene. M: size marker, 1: (Control): no p-AuNP, 2: OD450=2.484, 3: OD450=1.242, 4: OD450=0.621, 5: OD450=0.3105, 6: OD450=0.15525, 7: OD450=0.077625, 8: OD450=0.0388125, 9: OD450=0.01940625, 10: OD450=0.009703125.

By comparing the effect of p-AuNPs on the DNA samples with different GC contents, it could be suggested that an increase in the GC content is directly related to the PCR-enhancing effect of the

In other words, p-AuNPs showed a more intense effect in amplification of GC-rich DNA samples. In order to further confirm this hypothesis and quantify the observed effects, real-time PCR was performed.

Similar to the results of end-point PCR, real-time PCR amplification of mecA gene did not reveal any significant effect on the Ct of reactions containing serial concentrations of p-AuNPs as compared with the control reaction (figure 8).

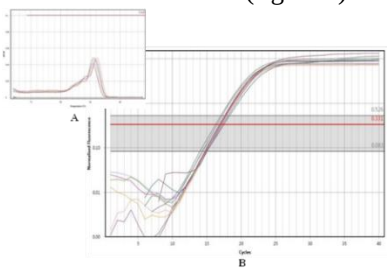

Figure 8. Effect of various concentrations of p-AuNPs on real-time PCR of mecA gene. The p-AuNPs did not show any significant effect on the specificity (A) and rate of the amplification (B).

For beta-actin in comparison to the control, marked decreases of approximately 1 and 3.5 cycles in the threshold cycle (Ct) was observed for p-AuNPs concentrations OD450=0.01940625 and OD450=0.009703125, respectively. This data confirms the results for end-point PCR, indicating 2- and 11.3-times enhancement in the amplification for the p-AuNPs concentrations used. Also, an evident improvement in the specificity of the primers was observed in the test reactions (figure 9).

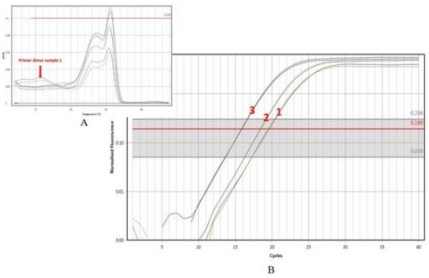

Figure 9. Effect of p-AuNPs on real-time PCR of the beta-actin gene. 1: control, 2: OD450=0.01940625, 3: OD450=0.009703125. Addition of the p-AuNPs improved the specificity of the reactions, as no primer dimer was observed in the test reactions (A). Also, a noticeable decrease was seen in the amplification curves (threshold cycles) of the reactions containing p-AuNP compared with the control reaction (B).

Similarly and as per the results of end-point PCR of BRAF gene, no DNA amplification was observed in the real-time PCR after 40 cycles in control and the reaction containing a high concentration of p-AuNPs. However, a Ct of near 25 and a Ct of 19 was detected in the reactions containing OD450=0.01940625 and OD450=0.009703125 concentrations of p-AuNPs, respectively. Further, the latter concentration showed approximately 64 times enhancement effect compared with the former concentration (figure 10).

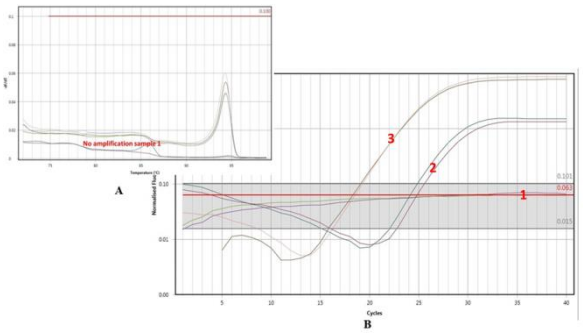

Figure 10. Effect of p-AuNPs on real-time PCR of BRAF gene. 1: control, 2: OD450=0.01940625, 3: OD450=0.009703125. From the melting curve (A) and the amplification curve (B) it is obvious that no amplification was occurred in the control reaction. However, a significant improvement of amplification is noticeable in the reactions received the p-AuNPs.

Overall the real-time PCR data are in agreement with the end-point PCR data concerning the relationship between GC % of target DNA and enhancing effect of p-AuNPs, showing a higher enhancing effect on the GC-rich DNA.

With regards to the results, p-AuNPs are capable of increasing the efficiency of PCR reactions in both end-point and real-time PCR reactions. The mechanism of this enhancement can be attributable to two main factors. The first one is that the metallic core of the nanoparticles is capable of heat transfer, which is homogenous due to the small and narrowly-distributed size of the p-AuNPs. In other words, p-AuNPs distribute the heat homogenously which, in turn, increases the efficiency of thermal cycling, leading to the production of a higher number of sequence copies. A similar mechanism has been reported for the chemically synthesized AuNPs [28].

The GC content-dependent nature of the PCR enhancement by p-AuNPs is in agreement with the significance of efficient heat transfer. As the GC content increases, the denaturation of double-strand template DNA requires more energy. Indeed, p-AuNPs show more effect on the templates with high GC content where they can be used to enhance the PCR efficiency.

The second factor can be related to the surface chemistry of p-AuNPs. As per the results, cit-AuNPs completely inhibit the PCR reactions. This inhibition is possibly due to the inactivation of components of the PCR reactions, particularly DNA polymerase, through the interaction of cit-AuNPs surface with these components [20]. The surface of cit-AuNPs is composed of citrate residues, containing hydroxyl and carboxyl groups, which form a fragile and heterogeneously distributed layer on the gold core. Particularly at the pH values greater than 5 these layers become loose, which is the pH of PCR reactions [29]; these factors make the gold core of cit-AuNPs easily accessible in PCR reactions. Furthermore, it has been shown that the thiol group has

a strong reaction with gold [30]. Thus, one main reason for inhibition of the PCR might be the interaction of the gold core of cit-AuNP with amino acids, especially thiol-contained amino acids, of DNA polymerase [31] such as Taq polymerase which contains 16 methionine groups [32], resulting in denaturation of the tridimensional structure of the polymerase.

Nevertheless, FTIR results show some different chemical residues on the surface of p-AuNPs and this layer is a relatively thick nanostructure, in contrary to the thin citrate layer of cit-AuNPs, which was originated from the bioreduction of the Au3+ anions by phenolic, protein and carbohydrate compounds of TEMC [33].

Although the size of both cit-AuNPs and p-AuNPs are similar, a 7 nm difference is observed in the wavelength of maximum absorbance between these AuNPs according to the UV-VIS analyses. This difference in the wavelength of maximum absorbance of these AuNPs indicates a red-shift in the LSPR curve of the p-AuNPs, revealing the presence of a relatively thick biological layer on the surface of the gold core. These organic compounds stabilize the p-AuNP spheres in pH of the PCR reaction, while this pH destabilizes cit-AuNP surface as mentioned above. It also serves as a barrier between the gold core and the components of the PCR reaction, keeping the gold core inaccessible to react with the reaction components. Therefore, p-AuNPs do not inactivate the Taq polymerase enzyme. Furthermore, the biocompatibility of these AuNPs, which has been confirmed by MTT assay, indicates an ambient interaction of these AuNPs with the biological moieties. On the other hand, cit-AuNPs possess cytotoxic effects on the cells that can be attributable to the formation of thiol-gold bonds with the biomolecules.

4. CONCLUSIONS

The PCR-enhancing effect of p-AuNPs can be used in many molecular biology reactions that need efficient heat transfer. In particular, p-AuNPs can increase the denaturation efficiency of high GC-content DNA, which in turn can increase the amplification rates of such DNA molecules. The successful amplification of high GC DNA, particularly real-time PCR, is necessary for the diagnosis of genetic diseases such as trinucleotide repeat disorders [34], and study of the molecular biology of some organisms that contain GC-rich genome such as Actinobacteria [35]. p-AuNP -as stable, biocompatible and cheap nanomaterial- can be a promising reagent for increasing the amplification rate of hard-to-amplify genetic material. With regards to the mechanisms involved in the enhancement of PCR reactions, other heat-dependent biological reactions can be enhanced by using p-AuNPs. Therefore, these p-AuNPs can be considered as a kit component for the commercial PCR master mixes.

5. REFERENCES

1. Baskaran, N.; Kandpal, R.P.; Bhargava, A.K.; Glynn, M.W.; Bale, A.; Weissman, S.M. Uniform amplification of a mixture of deoxyribonucleic acids with varying GC content. *Genome research* **1996,** *6*, 633-8.
2. McDowell, D.G.; Burns, N.A.; Parkes, H.C. Localised sequence regions possessing high melting temperatures prevent the amplification of a DNA mimic in competitive PCR. *Nucleic acids research* **1998,** *26*, 3340-7.
3. Frey, U.H.; Bachmann, H.S.; Peters, J.; Siffert, W. PCR-amplification of GC-rich regions: 'slowdown PCR'. *Nature protocols* **2008,** *3*, 1312-7, https://doi.org/10.1038/nprot.2008.112.
4. Don, R.H.; Cox, P.T.; Wainwright, B.J.; Baker, K.; Mattick, J.S. 'Touchdown' PCR to circumvent spurious priming during gene amplification. *Nucleic acids research* **1991,** *19*, 4008, https://doi.org/10.1093/nar/19.14.4008.
5. Hube, F.; Reverdiau, P.; Iochmann, S.; Gruel, Y. Improved PCR method for amplification of GC-rich DNA sequences. *Molecular biotechnology* **2005,** *31*, 81-4, https://doi.org/10.1385/MB:31:1:081.
6. Hecker, K.H.; Roux, K.H. High and low annealing temperatures increase both specificity and yield in touchdown and stepdown PCR. *BioTechniques* **1996,** *20*, 478-85, https://doi.org/10.2144/19962003478.
7. Lorenz, T.C. Polymerase chain reaction: basic protocol plus troubleshooting and optimization strategies. *Journal of visualized experiments : JoVE* **2012,** *63*, e3998, https://doi.org/10.3791/3998.
8. Pratyush, D.D.; Tiwari, S.; Kumar, A.; Singh, S.K. A new approach to touch down method using betaine as co-solvent for increased specificity and intensity of GC rich gene amplification. *Gene* **2012,** *497*, 269-72, https://doi.org/10.1016/j.gene.2012.01.031.
9. Zhang, Z.; Yang, X.; Meng, L.; Liu, F.; Shen, C.; Yang, W. Enhanced amplification of GC-rich DNA with two organic reagents. *BioTechniques* **2009,** *47*, 775-9. https://doi.org/10.2144/000113203.
10. Henke, W.; Herdel, K.; Jung, K.; Schnorr, D.; Loening, S.A. Betaine improves the PCR amplification of GC-rich DNA sequences. *Nucleic acids research* **1997,** *25*, 3957-8, https://doi.org/10.1093/nar/25.19.3957.
11. Sarkar, G.; Kapelner, S.; Sommer, S.S. Formamide can dramatically improve the specificity of PCR. *Nucleic acids research* **1990,** *18*, 7465, https://doi.org/10.1093/nar/18.24.7465.
12. Chakrabarti, R.; Schutt, C.E. The enhancement of PCR amplification by low molecular weight amides. *Nucleic acids research* **2001,** *29*, 2377-81, https://doi.org/10.1093/nar/29.11.2377.
13. Kang, J.; Lee, M.S.; Gorenstein, D.G. The enhancement of PCR amplification of a random sequence DNA library by DMSO and betaine: application to in vitro combinatorial selection of aptamers. *Journal of biochemical and biophysical methods* **2005,** *64*, 147-51, https://doi.org/10.1016/j.jbbm.2005.06.003.
14. Musso, M.; Bocciardi, R.; Parodi, S.; Ravazzolo, R.; Ceccherini, I. Betaine, dimethyl sulfoxide, and 7-deaza-dGTP, a powerful mixture for amplification of GC-rich DNA sequences. *The Journal of molecular diagnostics: JMD* **2006,** *8*, 544-50, https://doi.org/10.2353/jmoldx.2006.060058.
15. Yang, R.J.; Tseng, C.C.; Ju, W.J.; Fu, L.M.; Syu, M.P. Integrated microfluidic paper-based system for determination of whole blood albumin. *Sensors and Actuators B: Chemical* **2018**, *273*, 1091-1097, https://doi.org/10.1016/j.snb.2018.07.010.
16. Noh, Y.H.; Lee, S.; Whitaker, V.M.; Cearley, K.R; Cha, J.S. A high-throughput marker-assisted selection system combining rapid DNA extraction high-resolution melting and simple

sequence repeat analysis: Strawberry as a model for fruit crops. *Journal of Berry Research* **2017**, *7*, 23-31, https://doi.org/10.3233/JBR-160145.
17. Yeh, Y.C.; Creran, B.; Rotello, V.M. Gold nanoparticles: preparation, properties, and applications in bionanotechnology. *Nanoscale* **2012,** *4*, 1871-80, https://doi.org/10.1039/C1NR11188D.
18. Vu, B.V.; Litvinov, D.; Willson, R.C. Gold nanoparticle effects in polymerase chain reaction: favoring of smaller products by polymerase adsorption. *Analytical chemistry* **2008,** *80*, 5462-7, https://doi.org/10.1021/ac8000258.
19. Schill, W.B.; Galbraith, H.S. 37081. Detecting the undetectable: Characterization, optimization, and validation of an eDNA detection assay for the federally endangered dwarf wedgemussel, Alasmidonta heterodon (Bivalvia: Unionoida). *Aquatic conservation* **2019**, *29*, 603-611, https://doi.org/10.1002/aqc.3069.
20. Wan, W.; Yeow, J.T.; Van Dyke, M.I. Size-dependent PCR inhibitory effect induced by gold nanoparticles. *Conference proceedings : ... Annual International Conference of the IEEE Engineering in Medicine and Biology Society. IEEE Engineering in Medicine and Biology Society. Annual Conference* **2009,** *2009*, 2771-4, https://doi.org/10.1109/IEMBS.2009.5333865.
21. Kim, H.; Park, M.; Hwang, J.; Kim, J.; Chung, D.R.; Lee, K.S.; Kang, M. Development of label-free colorimetric assay for MERS-CoV using gold nanoparticles. *ACS sensors* **2019**, *4*, 1306-1312, https://doi.org/10.1021/acssensors.9b00175.
22. Dadashpour, M.; Firouzi-Amandi, A.; Pourhassan-Moghaddam, M.; Maleki, M.J.; Soozangar, N.; Jeddi, F.; Nouri, M.; Zarghami, N.; Pilehvar-Soltanahmadi, Y. Biomimetic synthesis of silver nanoparticles using Matricaria chamomilla extract and their potential anticancer activity against human lung cancer cells. *Materials science & engineering. C, Materials for biological applications* **2018,** *92*, 902-912, https://doi.org/10.1016/j.msec.2018.07.053.
23. Pourhassan-Moghaddam, M.; Zarghami, N.; Mohsenifar, A.; Rahmati-Yamchi, M.; Gholizadeh, D.; Akbarzadeh, A.; De La Guardia, M.; Nejati-Koshki, K. Watercress-based gold nanoparticles: biosynthesis, mechanism of formation and study of their biocompatibility in vitro. *Micro & Nano Letters* **2014,** *9*, 345-350, https://doi.org/10.1049/mnl.2014.0063.
24. Frias Batista, L.M.; Meader, V.K.; Romero, K.; Kunzler, K.; Kabir, F.; Bullock, A; Tibbetts, K.M. Kinetic Control of [AuCl4]− Photochemical Reduction and Gold Nanoparticle Size with Hydroxyl Radical Scavengers. *The Journal of Physical Chemistry B* **2019,** *123*, 7204-7213, https://doi.org/10.1021/acs.jpcb.9b04643.
25. Schumacher, A.; Vranken, T.; Malhotra, A.; Arts, J.J.C.; Habibovic, P. In vitro antimicrobial susceptibility testing methods: agar dilution to 3D tissue-engineered models. European *Journal of Clinical Microbiology & Infectious Diseases* **2018**, *37*, 187-208, https://doi.org/10.1007/s10096-017-3089-2.
26. Scanlan, L.D.; Coskun, S.H.; Jaruga, P.; Hanna, S.K.; Sims, C.M.; Almeida, J.L.; Catoe, D.; Coskun, E.; Golan, R.; Dizdaroglu, M.; Nelson, B.C. Measurement of Oxidatively-Induced DNA Damage in Caenorhabditis elegans with High-Salt DNA Extraction and Isotope-Dilution Mass Spectrometry. *Analytical chemistry* **2019,** *91*, 12149-12155, https://doi.org/10.1021/acs.analchem.9b01503.
27. Shore, S.; Paul, N. Robust PCR amplification of GC-rich targets with Hot Start 7-deaza-dGTP. *BioTechniques* **2010,** *49*, 841-843, https://doi.org/10.2144/000113552.
28. Wang, L.; Huang, Z.; Wang, R.; Liu, Y.; Qian, C.; Wu, J.; Liu, J. Transition metal dichalcogenide nanosheets for visual monitoring PCR rivaling a real-time PCR instrument. *ACS applied materials & interfaces* **2018,** *10*, 4409-4418, https://doi.org/10.1021/acsami.7b15746.
29. Park, J.W. Negative-Imaging of Citrate Layers on Gold Nanoparticles by Ligand-Templated Metal Deposition: Revealing Surface Heterogeneity. *Particle & Particle Systems Characterization* **2019,** *36*, 1800329, https://doi.org/10.1002/ppsc.201800329.
30. Heuer-Jungemann, A.; Feliu, N.; Bakaimi, I.; Hamaly, M.; Alkilany, A.; Chakraborty, I.; Masood, A.; Casula, M.F.; Kostopoulou, A.; Oh, E.; Susumu, K. The role of ligands in the chemical synthesis and applications of inorganic nanoparticles. *Chemical reviews* **2019**, *119*, 4819-4880, https://doi.org/10.1021/acs.chemrev.8b00733.
31. Guerrini, L.; Alvarez-Puebla, R.A.; Pazos-Perez, N. Surface modifications of nanoparticles for stability in biological fluids. *Materials* **2018,** *11*, 1154-1181, https://doi.org/10.3390/ma11071154.
32. Uniprot. https://www.uniprot.org/uniprot/P19821 (accessed 5 October 5, 2019).
33. Chaves, P.F.P.; Iacomini, M; Cordeiro, L.M. Chemical characterization of fructooligosaccharides, inulin and structurally diverse polysaccharides from chamomile tea. *Carbohydrate polymers* **2019**, *214*, 269-275, https://doi.org/10.1016/j.carbpol.2019.03.050.
34. Murmann, A.E.; Yu, J.; Opal, P.; Peter, M.E. Trinucleotide repeat expansion diseases, RNAi, and Cancer. *Trends in cancer* **2018**, *4*, 684-700, https://doi.org/10.1016/B978-0-444-63233-3.00009-9.
35. Tischler, D.; Van Berkel, W.J.; Fraaije, M.W. Actinobacteria, a Source of Biocatalytic Tools. *Frontiers in Microbiology* **2019**, *10*, 800, https://doi.org/10.3389/fmicb.2019.00800.

6. ACKNOWLEDGEMENTS

This article has been extracted from the Ph.D. thesis grant number “95/4-2/6”. The authors would like to thank the research deputy of Tabriz University of Medical Sciences for their financial support.